Journal of Molecular Modeling (2022) 28: 159
https://doi.org/10.1007/s00894-022-05160-5

ORIGINAL PAPER

# $S_N2$ versus E2 reactions in a complex microsolvated environment: theoretical analysis of the equilibrium and activation steps of a nucleophilic fluorination

**Fernando M. Lisboa**[1] · **Josefredo R. Pliego Jr.**[1]

Received: 18 February 2022 / Accepted: 12 May 2022 / Published online: 21 May 2022


**Abstract**
The reactivity of the fluoride ion towards alkyl halides is highly dependent on the solvating environment. In polar aprotic solvents with large counter-ions is highly reactive and produces substantial E2 product, whereas in polar protic solvents leads to slow kinetics and high selectivity for $S_N2$ reactions. The use of a more complex environment with stoichiometric addition of *tert*-butanol to acetonitrile solvent is able to module the reactivity and selectivity of tetrabutylammonium fluoride (TBAF). In the present work, we have performed a detailed theoretical analysis of this complex reaction system by density functional theory, continuum solvation model, and including explicit *tert*-butanol molecules. A kinetic model based on the free energy profile was also used to predict the reactivity and selectivity. The results indicated that the TBAF(*tert*-butanol) complex plays the key role to increase the $S_N2$ selectivity, whereas higher aggregates are not relevant. The E2 product is formed exclusively via free TBAF, because the solvating *tert*-butanol in the TBAF(*tert*-butanol) complex inhibits the E2 pathway. Our analysis suggests that diols or tetraols could produce an improved selectivity.

**Keywords** Solvent effects · Nucleophilic fluorination · DFT calculation · Microkinetic · Free energy profile · Cluster-continuum

## Introduction

The solvent effect on chemical reactions has a long history in chemistry [1, 2]. Solvents are widely used for improving reaction yield and can be critical for a successful reaction [2]. In the present time, the inclusion of solvent effects is mandatory for reliable modeling of condensed phase reactions. Indeed, with the development of theoretical methods and practical solvation models based on the continuum approach [3–8], fast theoretical solvent screening has become possible [9]. This approach has been applied for interesting problems such as solvent selection for some chemical reactions [10, 11] and separation processes via extraction [12, 13]. However, continuum solvation models have limitations and are not adequate for modeling reactions in situations that microsolvation plays a role [14–16], neither describing the solvation of many ionic species in protic solvents [17, 18]. In these cases, inclusion of explicit solvent is essential [19].

Among the different reaction types with important solvent effects, ion–molecule $S_N2$ and E2 reactions can be singled-out [20]. The first solvating shell has the main influence on these reactions. Thus, the microenvironment around the solute can be used for controlling the reaction rate and selectivity [21]. These ideas have led to the design of supramolecular catalysts for nucleophilic fluorination, mainly based on macrocycles such as crown ethers [22–25], cryptands [26, 27], calixarenes [28–31], thiourea-crown-ether [32], and similar structures [33–35].

Some years ago, Kim and co-workers [36, 37], followed by Gouverneur and co-workers [38], have reported the use of tetrabutylammonium fluoride (TBAF) in acetonitrile solvent and added stoichiometric amount of bulky alcohols as *tert*-butanol for performing nucleophilic fluorination. They observed an important effect of *tert*-butanol on the selectivity of the reaction. In fact, it is long known that fluoride

This paper belongs to Topical Collection: *XXI-Brazilian Symposium of Theoretical Chemistry (SBQT2021).*

✉ Josefredo R. Pliego Jr.
pliego@ufsj.edu.br

[1] Departamento de Ciências Naturais, Universidade Federal de São João del-Rei, São João del-Rei, MG 36301-160, Brazil

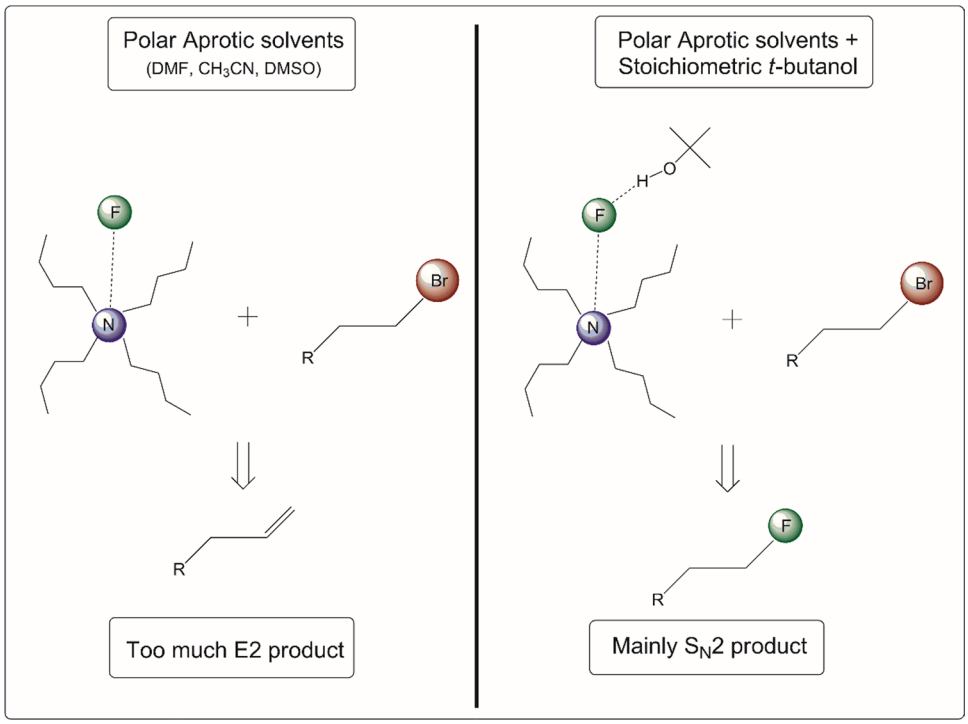


**Scheme 1** Microsolvation effect of the reaction selectivity. In the present study, R = H

ion in aprotic solvents can act as strong base, reacting with alkyl halides to generate much E2 product and decreasing the $S_N2$ yield [39, 40]. With the addition of stochiometric amount of molecules with hydroxyl groups such as water [41] or bulky alcohols [37, 38], a substantial increase of the $S_N2$ product is observed. However, the microscopic details on how the additional bulky alcohols combined with TBAF control the reaction rate and selectivity were not reported to date. Thus, the aim of this report is to conduct a theoretical analysis of this reaction system to provide more insights on the detailed mechanism. As a model system, we have used the ethyl bromide substrate reacting with TBAF and including up to three explicit *tert*-butanol molecules. Such problem involves modeling the reaction in a complex microsolvated environment [42]. We hope that this analysis can be useful for inducing more advances in the design of nucleophilic fluorination reactions.

## Theoretical methods

The reaction system presented in Scheme 1 was investigate by electronic structure calculations and continuum solvation (acetonitrile solvent), also including explicit *tert*-butanol molecules. Geometry optimization calculations of the minima and transition states investigated in this work were done using density functional theory method, with the PBE functional [43] and resolution of identity approximation. These calculations were performed with the ma-def2-SVP basis set [44, 45]. The optimizations were followed by harmonic frequency calculations to obtain thermodynamics data. However, because ORCA 3 program [46, 47] used in this study does not include frequencies below of 35 $cm^{-1}$ in the calculation of thermodynamics properties, which can lead to unbalanced description of the system, these contributions were included manually [48]. Additional correction for symmetry number and from standard state from 1 atm to 1 mol $L^{-1}$, necessary for modeling liquid phase processes, were also done. To obtain reliable free energies, the accurate M06-2X functional [49] with the extended ma-def2-TZVPP basis set was used for single point energy calculation. It is worth to observe that this functional was ranked among the top 10% better functionals for activation barrier and reaction energies in a recently comparative study involving 200 functionals [50].

The bulk solvent effect (acetonitrile) was included by the continuum SMD model [6]. This part of the calculations was done with the GAMESS program [51], using the X3LYP functional [52] and the 6–31(+)G(d) basis set. The final free energy for each species X in solution phase can be written as:

$$G_{sol}(X) = E_{el}(X) + G_N(X) + \Delta G_{solv}(X) \quad (1)$$

where the term in the left side is the free energy in liquid phase; the first term in the right side is the electronic energy obtained at M06-2X level; the second term is translational, rotational, and vibrational contribution to the free energy;

and the third term is the solvation free energy in acetonitrile. The $G_N$ term includes the correction for the standard state of 1 $mol^{-1}$. All calculations were performed with the ORCA 3 [46, 47] and GAMESS program [51] systems.

## Results and discussion

Previous work of our group involving tetramethyl ammonium fluoride (TMAF) in a similar polar aprotic solvent dimethylformamide has indicated that the $S_NAr$ reaction proceeds via ion pair [53]. In this report, the presence of TBAF and stoichiometric amount of *tert*-butanol in acetonitrile solution should lead to the formation of aggregates of the kind TBAF(t-butanol)$_N$, like that reported for a similar system: KF complexed with 18-crown-6 in acetonitrile solution with stoichiometric *tert*-butanol [24]. In that study, both molecular dynamics calculations and quantum chemistry with continuum solvation calculations have provide the same picture, which one *tert*-butanol molecule associated with the fluoride ion is the main species. Thus, the present theoretical approach for this system must provide a realistic picture of the problem under investigation.

The first part of the study was to analyze the formation of aggregates of TBAF with *t*-butanol. The optimized structures of TBAF interacting with up to three *t*-butanol molecules are presented in the Fig. 1. We can notice that the TBAF supports three *t*-butanol molecules solvating the fluoride ion in the first solvation shell. Although these structures are minima, only the complex with one *t*-butanol has a favorable ΔG for its formation. This thermodynamics data is presented in the Fig. 2, the free energy profile of the $S_N2$ reaction. Thus, TBAF(*t*-butanol) is only 0.6 kcal $mol^{-1}$ below of the TBAF + *t*-butanol reference. The complex with two *t*-butanol molecules is 2.0 kcal $mol^{-1}$ above of the free reactants and reaches 3.6 kcal $mol^{-1}$ for the complex with three *t*-butanol molecules. These are slightly negative and positive ΔG, indicating that all these species, including free TBAF, can be present in the equilibrium. The exact concentration of each species depends on the concentration of the added *t*-butanol. Because it is not clear the $\Delta G^{\ddagger}$ for each complex, all the species were included in the analysis.

In the activation step, the TBAF can react with ethyl bromide via four $S_N2$ transition states and four E2 transition states (Fig. 1). The direct reaction of TBAF with ethyl bromide has $\Delta G^{\ddagger} = 22.9$ kcal $mol^{-1}$ for both $S_N2$ and E2 pathways (Figs. 2 and 3). This finding indicates that both the fluorination and elimination products are formed in 50% selectivity, in agreement with experimental observations of high E2 product (22% $S_N2$: 78% E2, using true anhydrous TBAF) [37]. Consequently, the sole TBAF is not a good reactant for selective fluorination of alkyl halides [54]. With the participation of one *t*-butanol molecule, the free energy profile has an important modification. The free energy of the $S_N2$ pathway becomes 21.7 kcal $mol^{-1}$, whereas the free energy for the E2 pathway becomes 27.3 kcal $mol^{-1}$. These values correspond to the overall ΔG and consider the initial reactants as reference. Thus, the inclusion of just one *t*-butanol has an important effect on the selectivity and would be able to produce exclusively $S_N2$ product. Nevertheless, the reaction leading to E2 via free TBAF remains competitive (22.9 kcal $mol^{-1}$) and any conclusion on the observed selectivity requires a complete analysis of the equilibrium and kinetics.

The addition of the second *t*-butanol rises the ΔG of the $S_N2$ transition state to 27.5 kcal $mol^{-1}$, turning the kinetics by this pathway too slow. The third *t*-butanol molecule makes the free energy even higher, 31.9 kcal $mol^{-1}$. In the case of E2 pathway, the addition of the second and third *t*-butanol molecules also produces barriers above of 27 kcal $mol^{-1}$ (Fig. 3). Consequently, reaction kinetics via these transition states with two or three *t*-butanol molecules are slow and should not contribute meaningfully to the overall reaction rate and selectivity. However, it is important to observe that increasing the concentration of *t*-butanol produces more complexes, decreasing the concentration of free TBAF. This fact should improve the selectivity. In the next section, a detailed kinetics analysis is presented.

In order to ensure that the PBE/ma-def2-SVP geometries are enough to produce reliable barriers at M06-2X level, we have done additional M06-2X/ma-def2-SVP geometry optimizations for the species involved in the activation step of the $S_N2$ reaction involving TBAF(*t*-butanol), followed of single point energy calculation at M06-2X/ma-def2-TZVPP level. We have found that $\Delta E^{\ddagger}$ is 11.9 kcal $mol^{-1}$ using the PBE geometries and becomes 12.7 kcal $mol^{-1}$ using M06-2X geometries. This result supports the good quality of the present calculations.

### Analysis of the complexation equilibrium and reaction kinetics

In order to obtain more detailed and clearer view of the effect of *t*-butanol addition to the reaction system, the equilibria and kinetics equations with the free energy data from Figs. 2 and 3 were resolved. Thus, the equilibrium equations for formation of the complexes are given by:

$$K_1 = \frac{[\text{TBAF(tboh)}]}{[\text{TBAF}][\text{tboh}]} = e^{-\Delta G_1/RT} = 2.7 \quad (2)$$

$$K_2 = \frac{[\text{TBAF(tboh)}_2]}{[\text{TBAF}][\text{tboh}]^2} = e^{-\Delta G_2/RT} = 3.4 \times 10^{-2} \quad (3)$$

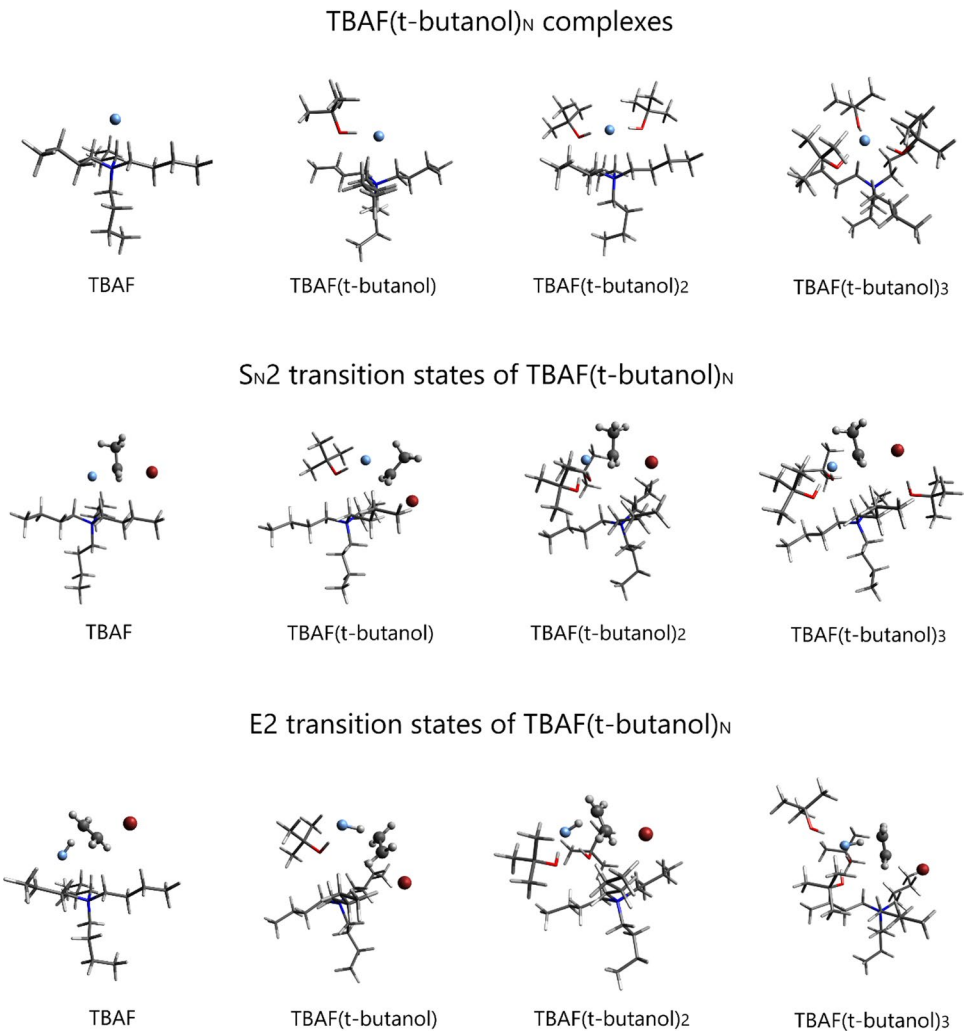


**Fig. 1** Minima and transition states structures of TBAF reaction with ethyl bromide in the presence of stoichiometric *t*-butanol obtained by the PBE/ma-def2-SVP method

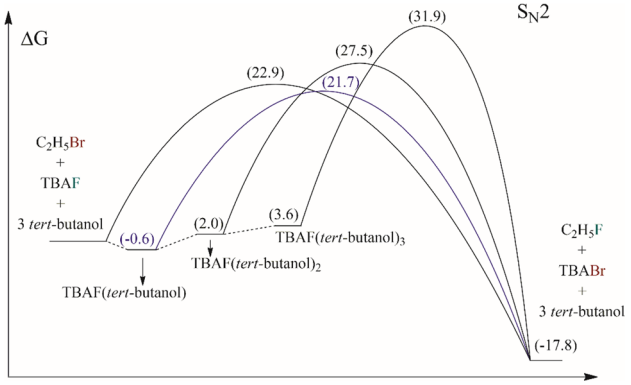


**Fig. 2** Free energy profile for the nucleophilic fluorination reaction ($S_N2$) of ethyl bromide with tetrabutylammonium fluoride in acetonitrile solvent and in the presence of *tert*-butanol. Units in kcal $mol^{-1}$. Standard state of 1 mol $L^{-1}$, 298.15 K. Calculations at M06-2X/ma-def2-TZVPP//X3LYP/ma-def2-SVP level and SMD solvation

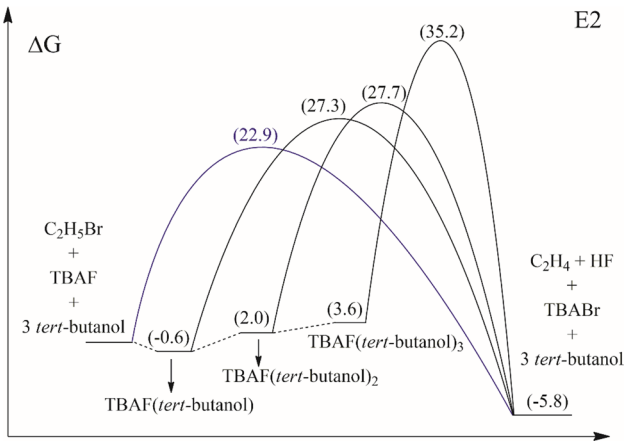


**Fig. 3** Free energy profile for the elimination reaction (E2) of ethyl bromide with tetrabutylammonium fluoride in acetonitrile solvent and in the presence of *tert*-butanol. Units in kcal $mol^{-1}$. Standard state of 1 mol $L^{-1}$, 298.15 K. Calculations at M06-2X/ma-def2-TZVPP//X3LYP/ma-def2-SVP level and SMD solvation

$$K_3 = \frac{[TBAF(tboh)_3]}{[TBAF][tboh]^3} = e^{-\Delta G_3/RT} = 2.3 \times 10^{-3} \quad (4)$$

and the mass balance requires:

$$C_{t\text{-butanol}} = [tboh] + [TBAF(tboh)] + 2.[TBAF(tboh)_2] + 3.[TBAF(tboh)_3] \quad (5)$$

$$C_{TBAF} = [TBAF] + [TBAF(tboh)] + [TBAF(tboh)_2] + [TBAF(tboh)_3] \quad (6)$$

where $C_{TBAF}$ and $C_{t\text{-butanol}}$ correspond to the total (analytic) concentration of TBAF and t-butanol, respectively, and tboh = *t*-butanol. The system of Eqs. (2) to (6) (five equations and five incognitos) was resolved using Excel with the conditions: $C_{TBAF} = 0.50$ mol $L^{-1}$, and $C_{t\text{-butanol}}$ was varied from 0.0 to 2.0 mol $L^{-1}$ to evaluate the concentration effect. The results are presented in the Fig. 4a. We can observe that the increase of $C_{t\text{-butanol}}$ up to 2.0 mol $L^{-1}$ leads to decrease of the concentration of free TBAF (close to 0.1 mol $L^{-1}$) and the increase of the concentration of the TBAF(t-butanol) up to 0.4 mol $L^{-1}$. The higher complexes have concentrations calculated to be below of 0.01 mol $L^{-1}$ even when using 2.0 mol $L^{-1}$ of $C_{t\text{-butanol}}$ and were not included in the graphics. As a consequence of this analysis, the E2 product should decrease with the increase of $C_{t\text{-butanol}}$, because this pathway must proceed via free TBAF.

In the kinetics analysis, we consider the pathways involving TBAF and TBAF(t-butanol) for $S_N2$ process, and TBAF for E2 because the free energy profile indicates that other pathways have remarkably high barriers (Figs. 2 and 3). Thus, the reaction rates are:

$$Rate_{SN2} = k_{0-SN2}[RBr][TBAF] + k_{1-SN2}[RBr][TBAF(tboh)] \quad (7)$$

$$Rate_{E2} = k_{0-E2}[RBr][TBAF] \quad (8)$$

With $k_{0\text{-}SN2}$ and $k_{0\text{-}E2}$ related to $\Delta G^{\ddagger} = 22.9$ kcal $mol^{-1}$ and $k_{1\text{-}SN2}$ related to $\Delta G^{\ddagger} = 21.7 - (-0.6) = 22.3$ kcal $mol^{-1}$. Based on this data calculated at 25 °C, we can predict that the selectivity of the $S_N2$ product is given by Fig. 4b. In this analysis, we are considering 100% conversion with the rate given by Eqs. (7) and (8). In the case that [*t*-butanol] = 0, there is 50% selectivity of the $S_N2$ product. Increasing the analytic concentration of *t*-butanol leads to increase of the selectivity up to 93% when $C_{t\text{-butanol}} = 2.0$ mol $L^{-1}$, and the graphics suggest a plateau at this concentration. This occurs because there is increase of the concentration of [TBAF(t-butanol)], resulting in low concentration of free TBAF able to react via E2. For comparison, the experiments of Gouverneur and co-workers have used $C_{RBr} = 0.25$ mol $L^{-1}$, $C_{TBOH} = 0.50$ mol $L^{-1}$ and $C_{t\text{-butanol}} = 2.0$ mol $L^{-1}$ and observed 67% selectivity using a primary alkyl bromide [38]. However, in [*t*-butanol] = 0 conditions, the experimental selectivity is only 22% [37]. Thus, this important increase in the selectivity is well reproduced in our calculations. The exact value is difficult to reproduce because this is a complex system, and the theoretical methods have limitations in the description of the solvation effect.

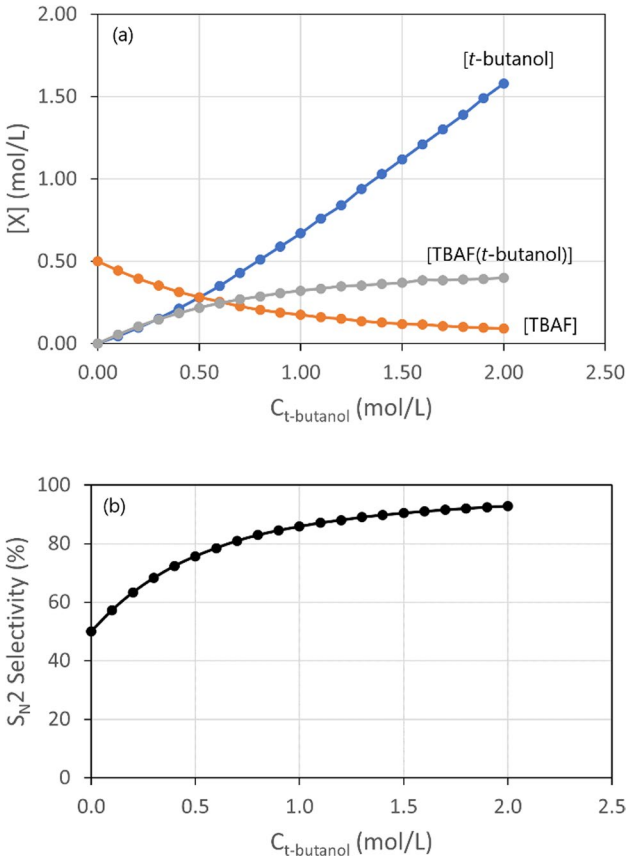


**Fig. 4** Effect of the total concentration of *t*-butanol on the concentration of each species (**a**) and on the selectivity (**b**) based on the theoretical free energy profile from Figs. 2 and 3

Further comparison can be done. Thus, our total reaction rate corresponds to $3.26 \times 10^{-5}$ mol $L^{-1}$ $s^{-1}$ using the experimental conditions. Defining a pseudo-second-order rate constant as suggested by Gouverneur and co-workers [38], given by:

$$Rate_{total} = k_t C_{RBr} C_{TBAF} \quad (9)$$

leads to $k_t = 2.61 \times 10^{-4}$ $M^{-1}$ $s^{-1}$, which corresponds to $\Delta G^{\ddagger} = 22.3$ kcal $mol^{-1}$ at 25 °C. The experiments of Gouverneur have resulted in $\Delta G^{\ddagger} = 23.1$ kcal $mol^{-1}$ at 70 °C. This is a particularly good agreement between theory and experiments. Thus, the present study provides a realist description of this complex system.

Based on the present results, the addition of *t*-butanol leads to the formation of TBAF(t-butanol) complex. Increasing the concentration of *t*-butanol does not produce appreciable concentration of higher aggregates such as TBAF(*t*-butanol)$_2$ or TBAF(*t*-butanol)$_3$, neither the reaction takes

place via these higher aggregates. Thus, improving the selectivity of $S_N2$ fluorination with adequate reaction rate could be achieved with the use of diols or tetraols with the right position of hydroxyls [23]. Such approach may lead to higher reaction rate and selectivity if stable aggregates, able to inhibit the reaction, are not formed.

## Conclusion

The present theoretical study indicates that micro-heterogeneous environment in the solution of TBAF dissolved in acetonitrile with stoichiometric *tert*-butanol has an important effect on the selectivity in the reaction of TBAF with alkyl bromide. There is considerable formation of the TBAF(t-butanol) complex, which react selectively with alkyl bromide to produce $S_N2$ product. The free TBAF in equilibrium is responsible for formation of the E2 product. The increase of the concentration of *t*-butanol does not lead to appreciable formation of higher aggregates. Rather, its effect is reducing the free TBAF species, decreasing the E2 product. Our analysis suggests that further improvement in the selectivity and reaction rate could be achieved with the use of diols or tetraols.

**Supplementary information** The online version contains supplementary material available at https://doi.org/10.1007/s00894-022-05160-5.

**Author contribution** Josefredo R. Pliego Jr. contributed to the study conception and design. Material preparation and data collection were performed by Fernando M. Lisboa. Analysis was performed by Fernando M. Lisboa and Josefredo R. Pliego Jr. The first draft of the manuscript was written by Josefredo R. Pliego Jr. and all authors commented on previous versions of the manuscript. All authors read and approved the final manuscript.

**Funding** The authors thank the agencies CNPq, FAPEMIG, and CAPES for support.

**Data availability** The datasets generated during and/or analyzed during the current study are available from the corresponding author on reasonable request.

**Code availability** Not applicable.

## Declarations

**Competing interests** The authors declare no competing interests.

## References

1. Reichardt C (2022) Solvation effects in organic chemistry: a short historical overview. J Org Chem 87:1616–1629
2. Reichardt C, Welton T (2011) Solvents and solvent effects in organic chemistry. Fourth edn. WILEY-VCH, Weinheim, Germany
3. Herbert JM (2021) Dielectric continuum methods for quantum chemistry. Wiley Interdiscip Rev Comput Mol Sci 11:e1519
4. Voityuk AA, Vyboishchikov SF (2020) Fast and accurate calculation of hydration energies of molecules and ions. Phys Chem Chem Phys 22:14591–14598
5. Klamt A (2018) The COSMO and COSMO-RS solvation models. Wiley Interdiscip Rev Comput Mol Sci 8:e1338
6. Marenich AV, Cramer CJ, Truhlar DG (2009) Universal solvation model based on solute electron density and on a continuum model of the solvent defined by the bulk dielectric constant and atomic surface tensions. J Phys Chem B 113:6378–6396
7. Tomasi J, Mennucci B, Cammi R (2005) Quantum mechanical continuum solvation models. Chem Rev 105:2999–3093
8. Lipparini F, Mennucci B (2016) Perspective: polarizable continuum models for quantum-mechanical descriptions. J Chem Phys 144:160901
9. Struebing H, Ganase Z, Karamertzanis PG, Siougkrou E, Haycock P, Piccione PM, Armstrong A, Galindo A, Adjiman CS (2013) Computer-aided molecular design of solvents for accelerated reaction kinetics. Nat Chem 5:952–957
10. Struebing H, Obermeier S, Siougkrou E, Adjiman CS, Galindo A (2017) A QM-CAMD approach to solvent design for optimal reaction rates. Chem Eng Sci 159:69–83
11. Dalessandro EV, Pliego JR Jr (2018) Solvent selection for chemical reactions: automated computational screening of solvents using the SMD model. Quim Nova 41:628–633
12. Dalessandro EV, Pliego JR Jr (2018) Fast screening of solvents for simultaneous extraction of furfural, 5-hydroxymethylfurfural and levulinic acid from aqueous solution using SMD solvation free energies. J Brazil Chem Soc 29:430–434
13. Blumenthal LC, Jens CM, Ulbrich J, Schwering F, Langrehr V, Turek T, Kunz U, Leonhard K, Palkovits R (2016) Systematic identification of solvents optimal for the extraction of 5-hydroxymethylfurfural from aqueous reactive solutions. ACS Sustain Chem Eng 4:228–235
14. Das M, Gogoi AR, Sunoj RB (2022) Molecular insights on solvent effects in organic reactions as obtained through computational chemistry tools. J Org Chem 87:1630–1640
15. Norjmaa G, Ujaque G, Lledós A (2021) Beyond continuum solvent models in computational homogeneous catalysis. Top Catal 65:118–140
16. Sunoj RB, Anand M (2012) Microsolvated transition state models for improved insight into chemical properties and reaction mechanisms. Phys Chem Chem Phys 14:12715–12736
17. Rufino VC, Pliego JR (2021) Single-ion solvation free energy: a new cluster-continuum approach based on the cluster expansion method. Phys Chem Chem Phys 23:26902–26910
18. Pliego JR Jr (2017) Cluster expansion of the solvation free energy difference: systematic improvements in the solvation of single ions. J Chem Phys 147:034104
19. Pliego JR Jr, Riveros JM (2020) Hybrid discrete-continuum solvation methods. Wiley Interdiscip Rev Comput Mol Sci 10:e1440
20. Anslyn EV, Dougherty DA (2006) Modern physical organic chemistry. University Science Books Sausalito, CA

21. Pliego JR (2021) The role of intermolecular forces in ionic reactions: the solvent effect, ion-pairing, aggregates and structured environment. Org Biomol Chem 19:1900–1914
22. Liotta CL, Harris HP (1974) Chemistry of naked anions. I. Reactions of the 18-crown-6 complex of potassium fluoride with organic substrates in aprotic organic solvents. J Am Chem Soc 96:2250–2252
23. Silva SL, Valle MS, Pliego JR (2020) Nucleophilic fluorination with KF catalyzed by 18-crown-6 and bulky diols: a theoretical and experimental study. J Org Chem 85:15457–15465
24. Silva SL, Valle MS, Pliego JR (2020) Micro-solvation and counter ion effects on ionic reactions: activation of potassium fluoride with 18-crown-6 and tert-butanol in aprotic solvents. J Mol Liq 319:114211
25. Jadhav VH, Jeong HJ, Choi W, Kim DW (2015) Crown ether metal complex fluoride salt as a facile and low hygroscopic fluoride source for nucleophilic fluorination. Chem Eng J 270:36–40
26. Schwesinger R, Link R, Wenzl P, Kossek S (2006) Anhydrous phosphazenium fluorides as sources for extremely reactive fluoride ions in solution. Chem Eur J 12:438–445
27. Pliego JR (2018) Potassium fluoride activation for the nucleophilic fluorination reaction using 18-crown-6, [2.2.2]-cryptand, pentaethylene glycol and comparison with the new hydro-crown scaffold: a theoretical analysis. Org Biomol Chem 16:3127–3137
28. Han HJ, Lee S-S, Kang SM, Kim Y, Park C, Yoo S, Kim CH, Oh Y-H, Lee S, Kim DW (2020) The effects of structural modifications of bis-tert-alcohol-functionalized crown-calix[4]arenes as nucleophilic fluorination promotors and relations with computational predictions. Eur J Org Chem 2020:728–735
29. Kang SM, Kim CH, Lee KC, Kim DW (2019) Bis-triethylene glycolic crown-5-calix[4]arene: a promoter of nucleophilic fluorination using potassium fluoride. Org Lett 21:3062–3066
30. Jadhav VH, Choi W, Lee S-S, Lee S, Kim DW (2016) Bis-tert-alcohol-functionalized crown-6-calix[4]arene: an organic promoter for nucleophilic fluorination. Chem Eur J 22:4515–4520
31. Pliego JR (2018) Mechanism of nucleophilic fluorination promoted by bis-tert-alcohol-functionalized crown-6-calix[4]arene. Int J Quantum Chem 118:e25648
32. Dalessandro EV, Pliego JR (2020) Theoretical design of new macrocycles for nucleophilic fluorination with KF: thiourea-crown-ether is predicted to overcome [2.2.2]-cryptand. Mol Syst Des Eng 5:1513–1523
33. Jadhav VH, Jang SH, Jeong H-J, Lim ST, Sohn M-H, Kim J-Y, Lee S, Lee JW, Song CE, Kim DW (2012) Oligoethylene glycols as highly efficient mutifunctional promoters for nucleophilic-substitution reactions. Chem Eur J 18:3918–3924
34. Lee JW, Yan H, Jang HB, Kim HK, Park SW, Lee S, Chi DY, Song CE (2009) Bis-terminal hydroxy polyethers as all-purpose, multifunctional organic promoters: a mechanistic investigation and applications. Angew Chem, Int Ed 48:7683–7686
35. Kim J-Y, Kim DW, Song CE, Chi DY, Lee S (2013) Nucleophilic substitution reactions promoted by oligoethylene glycols: a mechanistic study of ion-pair SN2 processes facilitated by Lewis base. J Phys Org Chem 26:9–14
36. Kim DW, Jeong H-J, Lim ST, Sohn M-H (2010) Facile nucleophilic fluorination of primary alkyl halides using tetrabutylammonium fluoride in a tert-alcohol medium. Tetrahedron Lett 51:432–434
37. Kim DW, Jeong H-J, Lim ST, Sohn M-H (2008) Tetrabutylammonium tetra(tert-butyl alcohol)-coordinated fluoride as a facile fluoride source. Angew Chem, Int Ed 47:8404–8406
38. Engle KM, Pfeifer L, Pidgeon GW, Giuffredi GT, Thompson AL, Paton RS, Brown JM, Gouverneur V (2015) Coordination diversity in hydrogen-bonded homoleptic fluoride-alcohol complexes modulates reactivity. Chem Sci 6:5293–5302
39. Cox DP, Terpinski J, Lawrynowicz W (1984) Anhydrous tetrabutylammonium fluoride - a mild but highly efficient source of nucleophilic fluoride-ion. J Org Chem 49:3216–3219
40. Landini D, Maia A, Rampoldi A (1989) Dramatic effect of the specific solvation on the reactivity of quaternary ammonium fluorides and poly(hydrogen fluorides), (Hf)-normal.F-, in media of low polarity. J Org Chem 54:328–332
41. Albanese D, Landini D, Penso M (1998) Hydrated tetrabutylammonium fluoride as a powerful nucleophilic fluorinating agent. J Org Chem 63:9587–9589
42. Maldonado AM, Basdogan Y, Berryman JT, Rempe SB, Keith JA (2020) First-principles modeling of chemistry in mixed solvents: where to go from here? J Chem Phys 152:130902
43. Perdew JP, Burke K, Ernzerhof M (1996) Generalized gradient approximation made simple. Phys Rev Lett 77:3865–3868
44. Zheng JJ, Xu XF, Truhlar DG (2011) Minimally augmented Karlsruhe basis sets. Theor Chem Acc 128:295–305
45. Weigend F, Ahlrichs R (2005) Balanced basis sets of split valence, triple zeta valence and quadruple zeta valence quality for H to Rn: design and assessment of accuracy. Phys Chem Chem Phys 7:3297–3305
46. Neese F, Wennmohs F, Becker U, Riplinger C (2020) The ORCA quantum chemistry program package. J Chem Phys 152:224108
47. Neese F (2012) The ORCA program system. Wiley Interdiscip Rev Comput Mol Sci 2:73–78
48. McQuarrie DA (2000) Statistical mechanics. University Science Books, Sausalito, CA
49. Zhao Y, Truhlar DG (2008) The M06 suite of density functionals for main group thermochemistry, thermochemical kinetics, noncovalent interactions, excited states, and transition elements: two new functionals and systematic testing of four M06-class functionals and 12 other functionals. Theor Chem Acc 120:215–241
50. Mardirossian N, Head-Gordon M (2017) Thirty years of density functional theory in computational chemistry: an overview and extensive assessment of 200 density functionals. Mol Phys 115:2315–2372
51. Barca GMJ, Bertoni C, Carrington L, Datta D, Silva ND, Deustua JE, Fedorov DG, Gour JR, Gunina AO, Guidez E, Harville T, Irle S, Ivanic J, Kowalski K, Leang SS, Li H, Li W, Lutz JJ, Magoulas I, Mato J, Mironov V, Nakata H, Pham BQ, Piecuch P, Poole D, Pruitt SR, Rendell AP, Roskop LB, Ruedenberg K, Sattasathuchana T, Schmidt MW, Shen J, Slipchenko L, Sosonkina M, Sundriyal V, Tiwari A, Vallejo JLG, Westheimer B, Włoch M, Xu P, Zahariev F, Gordon MS (2020) Recent developments in the general atomic and molecular electronic structure system. J Chem Phys 152:154102
52. Xu X, Zhang Q, Muller RP, Goddard WA III (2005) An extended hybrid density functional (X3LYP) with improved descriptions of nonbond interactions and thermodynamic properties of molecular systems. J Chem Phys 122:014105–014114
53. Dalessandro EV, Pliego JR (2020) Reactivity and stability of ion pairs, dimers and tetramers versus solvent polarity: SNAr fluorination of 2-bromobenzonitrile with tetramethylammonium fluoride. Theor Chem Acc 139:27
54. Sun H, DiMagno SG (2005) Anhydrous tetrabutylammonium fluoride. J Am Chem Soc 127:2050–2051